



Deposited via The University of Sheffield.

White Rose Research Online URL for this paper:

<https://eprints.whiterose.ac.uk/id/eprint/117966/>

Version: Accepted Version

Proceedings Paper:

Wang, J., Chu, X., Ding, M. et al. (2017) On the performance of multi-tier Heterogeneous networks under LoS and NLoS transmissions. In: 2016 IEEE Globecom Workshops (GC Wkshps). 2016 IEEE Globecom Workshops (GC Wkshps), 04-08 Dec 2016, Washington, DC, USA. IEEE. ISBN: 9781509024827.

<https://doi.org/10.1109/GLOCOMW.2016.7848983>

© 2016 IEEE. Personal use of this material is permitted. Permission from IEEE must be obtained for all other users, including reprinting/ republishing this material for advertising or promotional purposes, creating new collective works for resale or redistribution to servers or lists, or reuse of any copyrighted components of this work in other works. Reproduced in accordance with the publisher's self-archiving policy.

Reuse

Items deposited in White Rose Research Online are protected by copyright, with all rights reserved unless indicated otherwise. They may be downloaded and/or printed for private study, or other acts as permitted by national copyright laws. The publisher or other rights holders may allow further reproduction and re-use of the full text version. This is indicated by the licence information on the White Rose Research Online record for the item.

Takedown

If you consider content in White Rose Research Online to be in breach of UK law, please notify us by emailing eprints@whiterose.ac.uk including the URL of the record and the reason for the withdrawal request.

On the Performance of Multi-tier Heterogeneous Networks under LoS and NLoS Transmissions

Jiaqi Wang, Xiaoli Chu, Ming Ding* and David López-Pérez†

Department of Electronic & Electrical Engineering, University of Sheffield, Sheffield S1 3JD, UK

*Data61, CSIRO, Australia

†Nokia Bell Laboratories, Dublin, Ireland

Email: jwang25@sheffield.ac.uk, x.chu@sheffield.ac.uk, Ming.Ding@data61.csiro.au, dr.david.lopez@ieee.org

Abstract—Heterogeneous networks (HetNets) with a multi-tier structure have been considered as a promising method to provide high quality of service to mobile users. The dense deployment of small-cell base stations (BSs) implies short distances between BSs and users. It is therefore likely that users will see line-of-sight (LoS) links from its serving BS and even nearby interfering BSs, which has not been considered in performance analysis for multi-tier HetNets yet. In this paper, we study a dense multi-tier HetNet with LoS and non-line-of-sight (NLoS) transmissions based on a multi-slope path loss model. The spatial locations of BSs of any given network tier and those of mobile users are modeled as independent spatial Poisson point processes (SPPPs). We derive the expression of downlink coverage probability for the multi-tier HetNet, based on which we calculate the area spectral efficiency (ASE) and energy efficiency (EE) of the HetNet. Our analytical results demonstrate that in an extremely dense HetNet, both the ASE and EE of the HetNet will drop quickly with further increase of the small-cell density due to the dominance of LoS interfering small-cell links.

Index Terms—LoS, NLoS, HetNets, coverage probability, area spectral efficiency, energy efficiency.

I. INTRODUCTION

Dense deployments of small cells are widely considered as the most promising approach to provide high quality of service to mobile users. Thus, future cellular networks are likely to have a multi-tier structure composed of macrocell base stations (BSs) and overlaid small-cell BSs [1], [2], known as heterogeneous networks (HetNets). The small cells can be of various types, e.g., microcells, metrocells, picocells, or femtocells, and they can achieve large performance gains through aggressive spectrum reuse.

In many existing works, HetNets have been modeled as spatial Poisson point processes (SPPPs) for performance analysis. In [3], the coverage probability of a K -tier HetNet is analytically derived for both open and closed access schemes. The accuracy of SPPP modelling is evaluated by comparing its coverage probability with those of grid and real-world deployments. In [4], by taking advantage of the tractability offered by SPPP modeling, the authors show that a positive small-cell range expansion bias that encourages users to associate with lightly loaded small cells can enhance the HetNet coverage, and that this coverage can be optimized by tuning the density and bias factor of small cells. In [5], it has

been shown that the area spectral efficiency (ASE) of a HetNet increases with the increase of small-cell density when a single-slope path loss model is considered.

However, none of the above HetNet works has considered the possibility of line-of-sight (LoS) transmissions in the network. Although non-line-of-sight (NLoS) transmissions would usually occur in cellular communications, with the dense deployment of small-cell BSs and the resulting short distances between BSs and users, it is likely that users will see LoS links from its serving BS and even nearby interfering BSs. In [6], a multi-slope path loss model is used to model LoS and NLoS transmissions in a single-tier homogeneous small-cell network. The analytical results show both the existence of a maximum coverage probability and the non-linear increase or even decrease of the ASE with the small cell density. These probabilistic LoS transmissions have not been considered in the performance analysis for multi-tier HetNets yet. Moreover, in light of the results in [6], it is not clear whether or not the conclusions of HetNet coverage in [4] and ASE in [5] hold for a more comprehensive path loss model.

It is also worth noting that most HetNet performance analyses do not focus on energy efficiency (EE), and that a rapid increase in the number of deployed small-cell BSs may lead to an increase in the total energy consumption of a HetNet, affecting its environmental friendliness or economic sustainability [7]. Thus, there is a need for comprehensive HetNet performance analyses, considering also HetNet EE.

In this paper, we study the network performance of a dense multi-tier HetNet under a practical multi-slope path loss model that covers LoS and NLoS transmissions. The spatial locations of BSs of any given network tier and those of mobile users are modeled as independent SPPPs. A user is associated to the BS that offers the highest biased downlink received power, which is the downlink received power multiplied by the bias factor of the corresponding network tier. Under this practical yet tractable system model, we analyze and derive the expression of downlink coverage probability for a multi-tier HetNet, and then use it to calculate its ASE and EE. Numerical results are provided for a two-tier HetNet to verify the obtained analytical expressions and shed new light on the performance gains achievable by dense deployment of small cells in a HetNet.

The rest of the paper is organized as follows. In Section II, the system model is introduced. In Section III, we analyze the

coverage probability, ASE and EE for multi-tier HetNets under LoS and NLoS transmissions. In Section IV, we present the numerical results. In Section V, the conclusions are drawn.

II. SYSTEM MODEL

In this paper, we consider a K -tier ($K \geq 2$) HetNet with all the K tiers sharing the same frequency spectrum. The spatial distribution of the k^{th} tier BSs follows an independent homogeneous SPPP with intensity of $\lambda_k, k \in \{1, 2, \dots, K\}$. The indexes of all the k^{th} tier BSs are contained in the set Φ_k . The users are distributed over the K -tier HetNet area following another independent SPPP with intensity of λ_u , where λ_u is large enough to ensure that each BS has at least one user.

We use a multi-slope path loss model considering both LoS and NLoS transmissions as probabilistic events, where the path loss of a link is segmented into N slopes depending on the range of the link. Accordingly, the path loss between a k^{th} tier BS and a user at distance r is given by

$$l_k(r) = \begin{cases} l_{k,1}(r) = \begin{cases} l_{k,1}^L(r) = A_{k,1}^L r^{-\alpha_{k,1}^L} & \text{with } \Pr_1^L(r) \\ l_{k,1}^{\text{NL}}(r) = A_{k,1}^{\text{NL}} r^{-\alpha_{k,1}^{\text{NL}}} & \text{with } (1 - \Pr_1^L(r)) \end{cases} & 0 < r \leq d_1 \\ \vdots \\ l_{k,n}(r) = \begin{cases} l_{k,n}^L(r) = A_{k,n}^L r^{-\alpha_{k,n}^L} & \text{with } \Pr_n^L(r) \\ l_{k,n}^{\text{NL}}(r) = A_{k,n}^{\text{NL}} r^{-\alpha_{k,n}^{\text{NL}}} & \text{with } (1 - \Pr_n^L(r)) \end{cases} & d_{n-1} < r \leq d_n, \\ \vdots \\ l_{k,N}(r) = \begin{cases} l_{k,N}^L(r) = A_{k,N}^L r^{-\alpha_{k,N}^L} & \text{with } \Pr_N^L(r) \\ l_{k,N}^{\text{NL}}(r) = A_{k,N}^{\text{NL}} r^{-\alpha_{k,N}^{\text{NL}}} & \text{with } (1 - \Pr_N^L(r)) \end{cases} & r > d_{N-1} \end{cases} \quad (1)$$

where d_n ($n = 1, 2, \dots, N-1$) are the segment breaking points, $\Pr_n^L(r)$ ($n = 1, 2, \dots, N$) is the probability of LoS transmission of the n^{th} slope, $1 - \Pr_n^L(r)$ is the probability of NLoS transmission of the n^{th} slope, and $\alpha_{k,n}^L, \alpha_{k,n}^{\text{NL}}, A_{k,n}^L$ and $A_{k,n}^{\text{NL}}$ are the LoS and NLoS path loss exponents and path loss constants of the n^{th} slope in the k^{th} tier, respectively. 3GPP has suggested some expressions for $\Pr_n^L(r)$ [6].

Moreover, we consider a user association scheme based on the maximum biased received power [4], i.e.,

$$(i^*, k^*) = \arg \max_{k \in \{1, \dots, K\}, i \in \Phi_k} P_k B_k l_k(r_i), \quad (2)$$

where P_k and B_k are the transmit power and bias factor of a k^{th} tier BS, respectively, and r_i is the distance from the i^{th} BS in the k^{th} tier to the user.

Therefore, the user is associated to the $i^{*\text{th}}$ BS in the $k^{*\text{th}}$ tier¹, and the downlink signal-to-interference-plus-noise ratio (SINR) is given by

$$\text{SINR}_k(r_x) = \frac{P_k l_k(r_x) h_{r_x}}{I_{k,i} + N_0}, \quad (3)$$

where h_{r_x} is the channel fading power gain of the link between the i^{th} BS in the k^{th} tier and the user, which follows a unit-mean exponential distribution, $I_{k,i}$ is the interference power received from cross-tier and co-tier BSs and is expressed as

$$I_{k,i} = I_{\text{cross}} + I_{\text{co}} = \sum_{j=1}^K \sum_{x \in \Phi_j, j \neq k} P_j l_j(r_x) h_{r_x} + \sum_{x \in \Phi_k, x \neq i} P_k l_k(r_x) h_{r_x}, \quad (4)$$

and N_0 is the additive White Gaussian Noise (AWGN) power at the user.

III. PERFORMANCE ANALYSIS

In this section, we analyze the coverage probability of a multi-tier HetNet under the system model given in Section II, and then use the obtained coverage probability to calculate its ASE and EE.

A. Coverage Probability

The downlink coverage probability is defined as the probability that the downlink SINR of a user is above a pre-defined threshold [8], i.e.,

$$p_{\text{cov}} = \sum_{k=1}^K \mathbb{P}[\text{SINR}_k(r_i) > \gamma, k=k^*] \\ = \sum_{k=1}^K p_{\text{cov}_k}(\lambda_k, \gamma) \rho_k, \quad (5)$$

where $p_{\text{cov}_k}(\lambda_k, \gamma)$ is the coverage probability offered by the k^{th} tier [8], γ is the SINR threshold, and ρ_k , which is equal to $\mathbb{P}[k=k^*]$, is the probability of a typical user being associated with a k^{th} tier BS. Due to the page limitation, we omit the calculation of ρ_k and will present it in later version.

According to the multi-slope path loss model in (1), the coverage probability of a user associated with a k^{th} tier BS can be further expressed as

$$p_{\text{cov}_k}(\lambda_k, \gamma) = \sum_{n=1}^N (T_{k,n}^L + T_{k,n}^{\text{NL}}), \quad (6)$$

where the coverage probability of the n^{th} slope in the k^{th} tier is composed of the following two parts [6],

$$T_{k,n}^L = \int_{d_{n-1}}^{d_n} \mathbb{P}[\text{SINR}_k^L(r) > \gamma] f_{k,n}^L(r) dr \\ T_{k,n}^{\text{NL}} = \int_{d_{n-1}}^{d_n} \mathbb{P}[\text{SINR}_k^{\text{NL}}(r) > \gamma] f_{k,n}^{\text{NL}}(r) dr. \quad (7)$$

According to the computation in [6], SINR_k^L and $\text{SINR}_k^{\text{NL}}$ are the coverage probability offered by LoS and NLoS links, respectively, and are given by

$$\mathbb{P}[\text{SINR}_k^L(r) > \gamma] = \exp\left(-\frac{\gamma N_0 r^{\alpha_{k,n}^L}}{P_k A_{k,n}^L}\right) \prod_{j=1}^K \mathcal{L}_{I_{k,i}}\left(\frac{\gamma r^{\alpha_{k,n}^L}}{P_k A_{k,n}^L}\right) \\ \mathbb{P}[\text{SINR}_k^{\text{NL}}(r) > \gamma] = \exp\left(-\frac{\gamma N_0 r^{\alpha_{k,n}^{\text{NL}}}}{P_k A_{k,n}^{\text{NL}}}\right) \prod_{j=1}^K \mathcal{L}_{I_{k,i}}\left(\frac{\gamma r^{\alpha_{k,n}^{\text{NL}}}}{P_k A_{k,n}^{\text{NL}}}\right), \quad (8)$$

where $\mathcal{L}_j(s)$ is the Laplace transform of interference I_j [4]. The calculation of (8) is provided in Appendix A.

Moreover, $f_{k,n}^L(r)$ and $f_{k,n}^{\text{NL}}(r)$ are the probability density functions (PDF) of the link between a user and a k^{th} tier BS being LoS and NLoS, respectively, conditioned on the range r of the link satisfying $d_{n-1} < r \leq d_n$.

The expression of $f_{k,n}^L(r)$ is given by

¹ For brevity of notation, we omit ‘*’ from i^* and k^* hereafter.

$$f_{k,n}^L(r) = \frac{\Pr_n^L(r) 2\pi r \lambda_k}{\rho_k} \exp\left(-\int_0^r \Pr_n^L(u) 2\pi u \lambda_k du\right) \times \prod_{j=1, j \neq k}^K \exp\left(-\int_0^a \Pr_n^L(u) 2\pi u \lambda_j du\right) \times \prod_{j=1}^K \exp\left(-\int_0^b [1 - \Pr_n^L(u)] 2\pi u \lambda_j du\right), \quad (9)$$

where $a = \left(\frac{P_j B_j A_{j,n}^L}{P_k B_k A_{k,n}^L}\right)^{1/\alpha_{j,n}^L} r^{\alpha_{k,n}^L/\alpha_{j,n}^L}$ and $b = \left(\frac{P_j B_j A_{j,n}^{NL}}{P_k B_k A_{k,n}^{NL}}\right)^{1/\alpha_{j,n}^{NL}} r^{\alpha_{k,n}^L/\alpha_{j,n}^{NL}}$.

The calculation of (9) is provided in Appendix B.

The expression of $f_{k,n}^{NL}(r)$ is given by

$$f_{k,n}^{NL}(r) = \frac{(1 - \Pr_n^L(r)) 2\pi r \lambda_k}{\rho_k} \times \exp\left(-\int_0^r (1 - \Pr_n^L(u)) 2\pi u \lambda_k du\right) \times \prod_{j=1, j \neq k}^K \exp\left(-\int_0^c (1 - \Pr_n^L(u)) 2\pi u \lambda_j du\right) \times \prod_{j=1}^K \exp\left(-\int_0^d \Pr_n^L(u) 2\pi u \lambda_j du\right), \quad (10)$$

where $c = \left(\frac{P_j B_j A_{j,n}^{NL}}{P_k B_k A_{k,n}^{NL}}\right)^{1/\alpha_{j,n}^{NL}} r^{\alpha_{k,n}^{NL}/\alpha_{j,n}^{NL}}$ and $d = \left(\frac{P_j B_j A_{j,n}^L}{P_k B_k A_{k,n}^L}\right)^{1/\alpha_{j,n}^L} r^{\alpha_{k,n}^{NL}/\alpha_{j,n}^L}$.

By plugging (8), (9) and (10) into (7), we can calculate the coverage probability of LoS and NLoS links for the n^{th} slope in the k^{th} tier. By substituting the calculated (7), (6) and (15) into (5), we obtain the coverage probability of the K -tier.

B. Area Spectral Efficiency and Energy Efficiency

From [11], the ASE (in bit/s/Hz/m²) of a K -tier HetNet is the summation of the ASE offered by each tier, i.e.,

$$\text{ASE of all tiers} = \sum_{k=1}^K \lambda_k \log_2(1+\gamma) \rho_k p_{\text{cov}_k}(\lambda_k, \gamma). \quad (11)$$

Following [12], the EE (in bit/s/Hz/W) of the K -tier HetNet is defined as

$$\text{EE} = \frac{\text{ASE of all tiers}}{\sum_{k=1}^K \lambda_k P_k}, \quad (12)$$

where $\sum_{k=1}^K \lambda_k P_k$ is the average spatial power consumption [7]. By substituting (11) into (12), we have the EE of a K -tier as

$$\text{EE} = \frac{\sum_{k=1}^K \lambda_k \log_2(1+\gamma) \rho_k p_{\text{cov}_k}(\lambda_k, \gamma)}{\sum_{k=1}^K \lambda_k P_k}. \quad (13)$$

IV. NUMERICAL RESULTS

In this section, we present numerical results to verify the obtained analytical formulas based on a two-tier HetNet composed of macrocells and small cells, $K=2$. To simplify the numerical calculation, an unbiased network is considered, i.e., $B_1/B_2=1$, and we use a two-slope path loss model ($N=2$) in (1), with the LoS probability given as [6]

$$\Pr^L(r) = \begin{cases} 1 - \frac{r}{d_1} & \text{when } 0 < r \leq d_1 \\ 0 & \text{when } r > d_1 \end{cases}. \quad (14)$$

TABLE I: SIMULATION PARAMETERS

Parameter	Values
AWGN power	$N_0 = -95\text{dBm}$
d_1	300m
Macro BS transmit power	$P_1 = 53\text{dBm}$
Small-cell BS transmit power	$P_2 = 23\text{dBm}$
Bias factor ratio	$B_1/B_2 = 1$
Small scale fading gain	$h \sim \exp(1)$
LoS path loss exponent	$\alpha^L = 2.09$
NLoS path loss exponent	$\alpha^{NL} = 3.75$
LoS path loss constant	$A^L = 10^{-3.29}$
NLoS path loss constant	$A^{NL} = 10^{-4.11}$

Moreover, the path loss exponents and constants of each slope in each tier are assumed to be same, i.e., $\alpha_{k,n}^L = \alpha^L$, $\alpha_{k,n}^{NL} = \alpha^{NL}$, $A_{k,n}^L = A^L$ and $A_{k,n}^{NL} = A^{NL}$, i.e., $k, n \in \{1, 2\}$. Table I shows the parameter values used in the following.

A. Coverage Probability

Fig. 1 shows the coverage probability versus the SINR threshold for different small cell densities, where $\lambda_1 = 1/(250^2\pi)$. For a given ratio between λ_2 and λ_1 , the coverage probability decreases with the SINR threshold. This is because the coverage definition becomes more challenging. For a given SINR threshold, the coverage probability decreases with the ratio between λ_2 and λ_1 . This is because as the ratio between small cell density and macrocell density increases, it is more likely that a user will see LoS transmissions from nearby small-cell BSs. Since a LoS link causes much less attenuation of signal power than a NLoS link, the cross-tier interference caused by small cells to macrocells and the co-tier interference between small cells becomes more severe with the increase of λ_2 . Thus, the coverage probability decreases.

Fig. 2 shows the coverage probability versus the density of small cells for different macrocell densities, where the SINR threshold is 0dB. For a given density of small cells (less than 0.01 BSs per m²), the coverage probability increases with the density of macrocells. This is because a higher density of macrocells leads to a shorter average distance from a macro BS to a user, thus a higher macrocell coverage probability. For a given λ_1 , the coverage probability first increases with λ_2 and then decreases with it after reaching a maximum value. This is because at relatively low small-cell densities, small-cell links are likely to be NLoS and the small-cell link quality (thus coverage probability) increases with the small-cell density; while at relatively high small-cell densities, small-cell links are likely to be LoS and the interfering small-cell links become more dominant, leading to reduced coverage probability. It is interesting to note that for different values of λ_1 , the maximum coverage probability occurs at approximately the same value of λ_2 , i.e., 2×10^{-5} BS per m². At very high densities of small cells (larger than 0.01 BSs per m²), the coverage probabilities for different values of λ_1 converge to the same low value, because all links are LoS dominated.

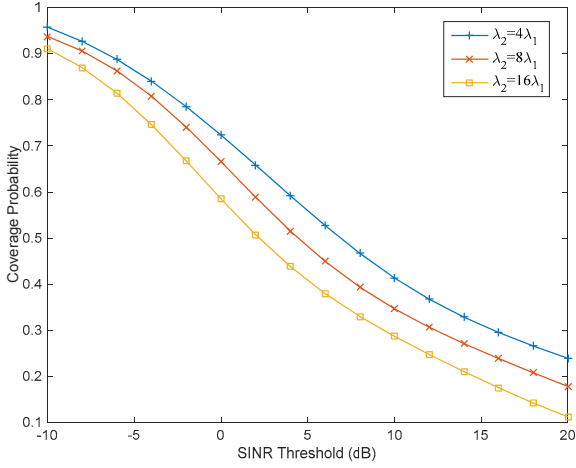


Fig. 1: Coverage probability vs. SINR threshold.

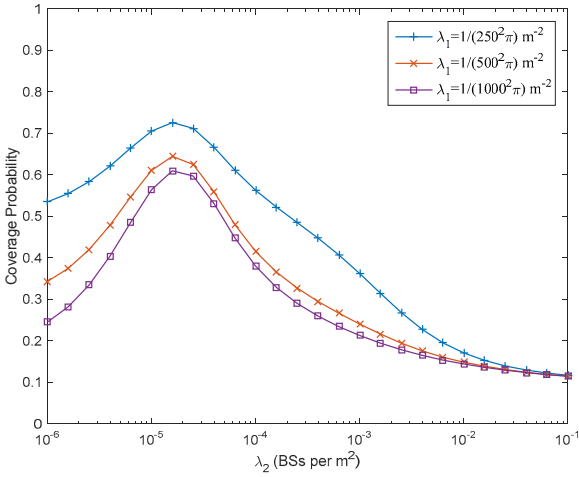


Fig. 2: Coverage probability vs. small-cell density for different macrocell densities.

B. Area spectral efficiency

In Fig. 3 and Fig. 4, we set $\lambda_1=1/(250^2\pi)$ and $\lambda_2=2\lambda_1$.

Fig. 3 shows the ASE and the EE of the two-tier HetNet versus the SINR threshold. As can be seen, the ASE of small cells first increases with the SINR threshold and then decreases with it after reaching a maximum value. This is mainly due to the NLoS-to-LoS transition of interference links as described in [6]. In contrast, the ASE of macrocells increases almost linearly with the SINR threshold, since such transition does not occur. Following (11), the ASE of the HetNet (as the summation of per-tier ASE) also first increases with the SINR threshold and then slowly decreases after reaching a maximum value. Given the parameters in Table I and above, the spatial power consumption is approximately 1 W/m^2 , and the EE is thus equal to the overall ASE.

Fig. 4 shows the ASE and the EE of the two-tier HetNet versus the transmit power of small cells, where the SINR threshold is 0dB. The ASE of macrocells increases slightly with the growth of small-cell BS transmit power, while the ASE of small cells slightly decreases, because the cross-tier

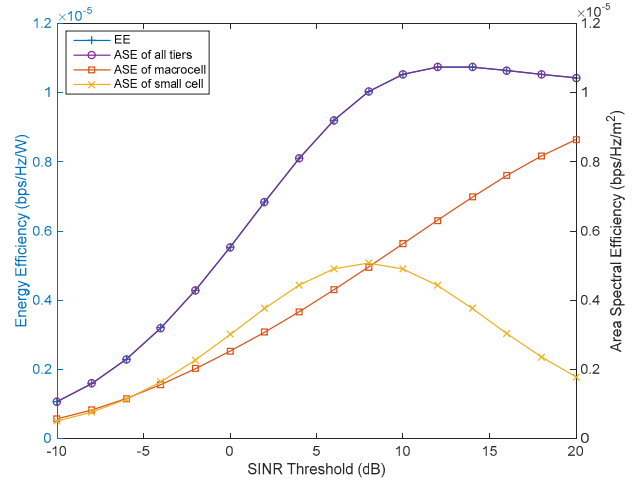


Fig. 3: ASE and EE vs. SINR threshold.

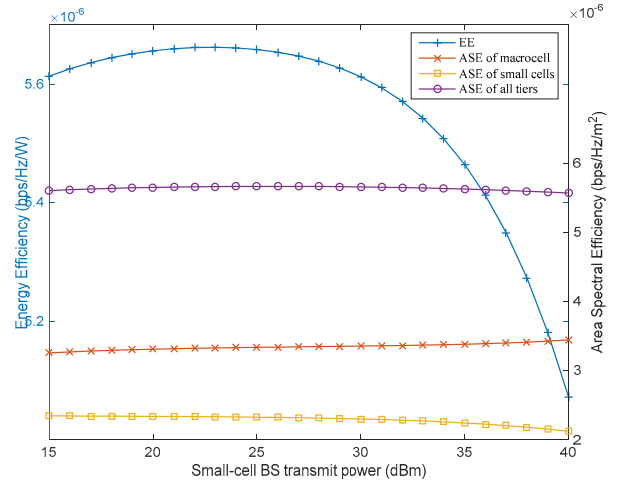


Fig. 4: ASE and EE vs. transmit power of small cells.

interference caused by small cells increases with the small-cell transmit power. As a result, the overall ASE of the HetNet is roughly constant over the different transmit power levels of small cells. Moreover, we observe that the EE of the HetNet first slightly increases with the small-cell transmit power and then drops quickly when the transmit power of small cells is above 25dBm. Thus, high transmit powers should be avoided for densely deployed small cells, because it will not improve the ASE but will degrade the EE significantly.

Fig. 5 compares the ASE of macrocells, small cells and all tiers calculated using our formula with those calculated in [4] versus λ_2 , for $\lambda_1=1/(250^2\pi)$. The SINR threshold is 0dB. In [4], no possible LoS transmission is considered and the path loss model follows $r^{-\alpha}$, where r is the link range and the path loss exponent $\alpha=4.5$. As Fig. 5 shows, both our formula and that in [4] predict that the ASE of small cells (macrocells) increases (decreases) with λ_2 at a smaller (higher) rate when λ_2 is larger than a certain value, but the value of λ_2 predicted by our calculations at which the increase rate of small-cell ASE reduces is smaller than that predicted by [4], while the value of λ_2 predicted by our formula at which the decrease rate of

macrocell ASE increases is larger than that predicted by [4]. This is because for the same low or moderate value of λ_2 , the inter-cell interference caused by small cells is severer with possible LoS transmissions than without. When λ_2 becomes extremely large, in contrary to the result of [4], the ASE of all tiers calculated by our formula decreases quickly with λ_2 , because the ASE of all tiers is now dominated by the small-cell ASE, which decreases quickly with λ_2 . This is because the domination of LoS transmissions in ultra-dense small-cell deployment results in extremely high inter-cell interference from small cells, which blocks most desired transmission links.

C. Energy efficiency

Fig. 6 shows the EE calculated by our formula and that calculated by [4] versus λ_2 for $\lambda_1=1/(250^2\pi)$, for a SINR threshold of 0dB and different path loss exponents. We can see that the highest EE is achieved with the smaller α^L and the larger α^{NL} at specific small cell densities. This is due to the fact that for such small cell densities, most interfering links are likely to be NLoS and only downlinks from serving BSs are possibly LoS, then for a small α^L and a large α^{NL} , the possibly LoS desired links would be strong while most interfering links would be relatively weak, thus leading to the highest EE.

For a small value of λ_2 ($<3\times 10^{-4}$ BSs per m^2), the lowest EE is obtained with the larger α^L and the smaller α^{NL} . This is because at low density of small cells, most interfering links are likely to be NLoS and only downlinks from serving BSs are possibly LoS, then for a large α^L and a small α^{NL} , any possible LoS desired links would be weak while most interfering links would be strong, resulting in the lowest EE.

For a moderate or large value of λ_2 (i.e., $3\times 10^{-4}<\lambda_2<1$ BSs per m^2), the lowest EE is obtained with the small α^L and the small α^{NL} . This is because for a relatively large density of small cells, most interfering small cell links are likely to be LoS while interfering macrocell links are likely to be NLoS, then with small values of α^L and α^{NL} , the interference caused by both small cells and macrocells becomes strong, leading to the lowest EE.

At extremely large values of λ_2 , our formula predicts that the EE decreases with the further increase of λ_2 , especially fast for the smaller value of α^L . This is because with densely deployed small cells, most small cell links are likely to be LoS, making the cross-tier and co-tier interference caused by small cells very strong (especially for a small α^L), and thus a higher λ_2 leads to a lower EE. However, such decrease of EE at extremely large λ_2 is not captured by formulas in [4].

In each considered pair of α^L and α^{NL} or for the given α , the EE increases very slightly with λ_2 at low or large values of λ_2 , but increases fast with λ_2 at moderate values of λ_2 . The reason is that as each small cell can serve only a small number of users, a moderate density of small cells is required to noticeably improve the overall network ASE (and thus EE).

V. CONCLUSION

Based on a multi-slope path loss model, we have derived the formulas of coverage probability, ASE and EE for a K -tier HetNet considering LoS and NLoS transmissions. Our

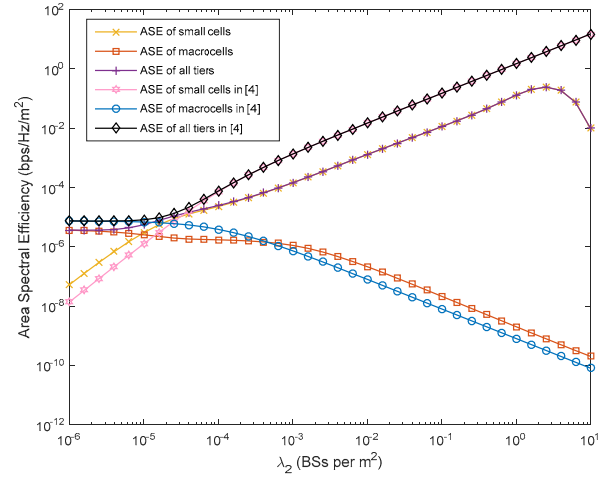


Fig. 5: ASE of macrocell and small cell vs. small cell density.

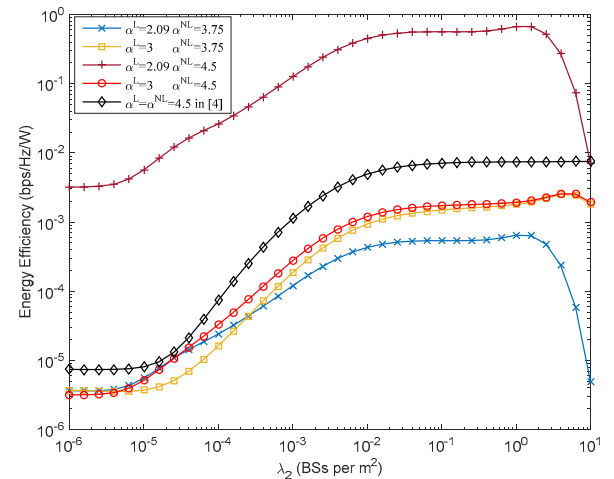


Fig. 6: EE vs. small cell density at different path loss exponents.

high small-cell densities, the transition of small cell interference links from NLoS to LoS will cause excessive inter-cell interference, which blocks almost all desired links. When small-cell BSs are densely deployed, increasing small-cell transmit power will not improve the ASE, but will degrade the EE significantly. Moreover, our results predict that in an extremely dense HetNet, both the ASE and EE of the HetNet will drop quickly with further increase of the small-cell density due to the dominance of LoS interfering links.

APPENDIX A

The probability of a downlink user with LoS transmission from the serving BS having SINR greater than the threshold γ is given by

$$\begin{aligned} \mathbb{P}[\text{SINR}_k^L(r) > \gamma] &= \mathbb{P}\left[\frac{P_{k,i}^L(r)h_{r_x}}{I_{k,i} + N_0} > \gamma\right] \\ &= \mathbb{E}_{I_{k,i}} \left\{ \mathbb{P}\left[h_{r_x} > \frac{\gamma(I_{k,i} + N_0)}{P_{k,i}^L(r)}\right] \right\} \end{aligned}$$

$$\begin{aligned}
& \text{(a)} \mathbb{E}_{I_{k,i}} \left\{ \exp \left(-\frac{\gamma(I_{k,i} + N_0)}{P_k l_{k,n}^L(r)} \right) \right\} \\
& \text{(b)} \exp \left(-\frac{\gamma N_0}{P_k l_{k,n}^L(r)} \right) \mathcal{L}_{I_{\text{co}}} \left(\frac{\gamma r^{\alpha_{k,n}^L}}{P_k A_{k,n}^L} \right) \\
& \prod_{j=1, j \neq k}^K \mathcal{L}_{I_{\text{cross}}} \left(\frac{\gamma r^{\alpha_{k,n}^L}}{P_k A_{k,n}^L} \right) \\
& = \exp \left(-\frac{\gamma N_0 r^{\alpha_{k,n}^L}}{P_k A_{k,n}^L} \right) \prod_{j=1}^K \mathcal{L}_{I_{k,i}} \left(\frac{\gamma r^{\alpha_{k,n}^L}}{P_k A_{k,n}^L} \right). \tag{15}
\end{aligned}$$

where (a) is based on exponential distributed power gain $h \sim \exp(1)$, and (b) follows the definition of Laplace transform of interference, $\mathcal{L}_I(s) = \mathbb{E}_I[\exp(-sI)]$.

APPENDIX B

The probability of a user being R_k away from its serving BS with the LoS link is regarded to r , which can be expressed by the combination of the probability of any LoS BS located outside the distance R_k^L and any NLoS BS located outside the distance R_k^{NL} conditioned on the probability of the LoS BS belonging to the k^{th} tier. The probability is given by

$$\begin{aligned}
\mathbb{P}[R_k > r] &= \mathbb{P}[R_k^L > r, R_k^{\text{NL}} > r | k = k^*] \\
&= \frac{\mathbb{P}[R_k^L > r, R_k^{\text{NL}} > r, k = k^*]}{\mathbb{P}[k = k^*]} \\
&= \frac{\mathbb{P}[X_k^L > r, X_k^{\text{NL}} > r, k = k^*]}{\rho_k}, \tag{16}
\end{aligned}$$

Where $\rho_k = \mathbb{P}[k = k^*]$, and the numerator is expressed as

$$\begin{aligned}
\mathbb{P}[R_k^L > r, R_k^{\text{NL}} > r, k = k^*] &= \int_r^\infty \mathbb{P}[R_k^L > r, R_k^{\text{NL}} > r] f_{R_k}(r) \\
&= \int_r^\infty \left\{ \prod_{j=1, j \neq k}^K \mathbb{P}[P_k B_k l_{k,n}^L(r) > P_j B_j l_{j,n}^L(x)] \right. \\
&\quad \left. \times \prod_{j=1}^K \mathbb{P}[P_k B_k l_{k,n}^L(r) > P_j B_j l_{j,n}^{\text{NL}}(x)] \right\} f_{R_k}(r) dr. \tag{17}
\end{aligned}$$

A. Computation of $f_{R_k}(r)$

The nearest BS with a LoS path to the user is located at R_k away from the user. The CCDF of R_k is

$$F_{R_k}(r) = \exp(-\int_0^r \text{Pr}_n^L(u) 2\pi u \lambda_k du). \tag{18}$$

The PDF of R_k is

$$f_{R_k}(r) = \exp(-\int_0^r \text{Pr}_n^L(u) 2\pi u \lambda_k du) \text{Pr}_n^L(r) 2\pi r \lambda_k. \tag{19}$$

B. Computation of $\mathbb{P}[P_k B_k l_{k,n}^L(r) > P_j B_j l_{j,n}^L(x)]$

The probability in (20) is calculated to be the probability of no BS being closer to the user than $\left(\frac{P_j B_j A_{j,n}^L}{P_k B_k A_{k,n}^L}\right)^{1/\alpha_{j,n}^L} r^{\alpha_{k,n}^L/\alpha_{j,n}^L}$ in the j^{th} tier,

$$\begin{aligned}
& \mathbb{P}[P_k B_k l_{k,n}^L(r) > P_j B_j l_{j,n}^L(x)] \\
&= \mathbb{P}\left[A_{k,n}^L r^{-\alpha_{k,n}^L} > \frac{P_j B_j}{P_k B_k} A_{j,n}^L x^{-\alpha_{j,n}^L}\right] \\
&= \mathbb{P}\left[x > \left(\frac{P_j B_j A_{j,n}^L}{P_k B_k A_{k,n}^L}\right)^{1/\alpha_{j,n}^L} r^{\alpha_{k,n}^L/\alpha_{j,n}^L}\right] \\
&= \exp\left(-\int_0^a \text{Pr}_n^L(u) 2\pi u \lambda_j du\right), \tag{20}
\end{aligned}$$

$$\text{where } a = \left(\frac{P_j B_j A_{j,n}^L}{P_k B_k A_{k,n}^L}\right)^{1/\alpha_{j,n}^L} r^{\alpha_{k,n}^L/\alpha_{j,n}^L}.$$

C. Computation of $\mathbb{P}[P_k B_k l_{k,n}^L(r) > P_j B_j l_{j,n}^{\text{NL}}(x)]$

Following similar computation of (20), we have

$$\mathbb{P}[P_k B_k l_{k,n}^L(r) > P_j B_j l_{j,n}^{\text{NL}}(x)] = \exp\left(-\int_0^b [1 - \text{Pr}_n^L(u)] 2\pi u \lambda_j du\right), \tag{21}$$

$$\text{where } b = \left(\frac{P_j B_j A_{j,n}^{\text{NL}}}{P_k B_k A_{k,n}^L}\right)^{1/\alpha_{j,n}^{\text{NL}}} r^{\alpha_{k,n}^L/\alpha_{j,n}^{\text{NL}}}.$$

From (19), (20) and (21) the CDF of R_k is $F_{k,n}^L(r) = (1 - \mathbb{P}[R_k > r])$. Thus, the PDF is shown as (9).

ACKNOWLEDGEMENT

This work was supported by the EC H2020 Project DECADE (MSCA-RISE-2014-645705).

REFERENCES

- [1] Z. Zheng, X. Zhang, L. X. Cai, R. Zhang and X. Shen, "Sustainable communication and networking in two-tier green cellular networks," *IEEE Wireless Commun.*, vol. 21, pp. 47-53, Aug. 2014.
- [2] H. Zhang, C. Jiang, N. Beaulieu, X. Chu, X. Wen and M. Tao, "Resource allocation in spectrum-sharing OFDMA femtocells with heterogeneous services," *IEEE Transactions on Communications*, vol. 62, no. 7, pp. 2366-2377, July 2014.
- [3] H. S. Dhillon, R. K. Ganti, F. Baccelli and J. G. Andrews, "Modeling and analysis of K-tier downlink heterogeneous cellular networks," *IEEE J. Sel. Areas Commun.*, vol. 30, no. 3, pp. 550-560, Apr. 2012.
- [4] H.-S. Jo, Y. J. Sang, P. Xia and J. G. Andrews, "Heterogeneous cellular networks with flexible cell association: a comprehensive downlink SINR analysis," *IEEE Trans. Wireless Commun.*, vol. 11, no. 10, pp. 3484-3495, Oct. 2012.
- [5] L. Yang, S. H. Song and K. B. Letaief, "Jointly optimal spectrum deployment and cognitive access for ASE maximization of macro-femto HetNets," *2015 IEEE International Conference (ICC)*, pp.100-105, 2015.
- [6] M. Ding, P. Wang, D. López-Pérez, G. Mao and Z. Lin, "Performance impact of LoS and NLoS transmissions in dense cellular networks," *IEEE Trans. Wireless Commun.*, vol. 15, no. 3, pp.2365-2380, Mar. 2016.
- [7] K. Davaslioglu, C. C. Coskun and E. Ayanoglu, "Energy-efficient resource allocation for fractional frequency reuse in heterogeneous networks," *IEEE Trans. Wireless Commun.*, vol. 14, no. 10, Oct. 2015.
- [8] A. K. Gupta, H. S. Dhillon, S. Vishwanath and J. G. Andrews, "Downlink coverage probability in MIMO HetNets with flexible cell selection," in *Proc., IEEE Globecom 2014*, pp. 1534-1539, 2014.
- [9] S. Hashima, O. Muta, M. Alghonimey, H. Shalaby, H. Frukawa, S. Elnoubi and I. Mahmoud, "Area spectral efficiency performance comparison of downlink fractional frequency reuse schemes for MIMO heterogeneous networks," *2012 IEEE International Conference (ISEEE)*, pp. 1005-1010, Apr. 2014.
- [10] Z. Zhang, Y. Li, S. Zhou and J. Wang, "Energy efficiency analysis of cellular networks with cooperative relays via stochastic geometry," *IEEE China Commun.*, vol. 12, pp. 112-121, Sep. 2015.
- [11] Y. Huang, X. Zhang, J. ZHANG, J. Tang, Z. Su and W. Wang, "Energy-efficient design in heterogeneous cellular networks based on large-scale user behavior constraints," *IEEE Trans. Wireless Commun.*, vol. 13, no. 9, pp. 4746-4757, Sep. 2014.
- [12] X. Zhang and J. G. Andrews, "Downlink cellular network analysis with multi-slope path loss models," *IEEE Trans. Commun.*, vol. 63, no. 5, pp. 1881-1894, May 2015.